NASA Technical Memorandum 110197

Fracture Analysis of Stiffened Panels Under Biaxial Loading with Widespread Cracking

J. C. Newman, Jr.
Langley Research Center, Hampton, Virginia

October 1995

National Aeronautics and
Space Administration
Langley Research Center
Hampton, Virginia 23681-0001

FRACTURE ANALYSIS OF STIFFENED PANELS UNDER BIAXIAL LOADING WITH WIDESPREAD CRACKING

J. C. Newman, Jr.
NASA Langley Research Center
Hampton, Virginia, USA

ABSTRACT

An elastic-plastic finite-element analysis with a critical crack-tip-opening angle (CTOA) fracture criterion was used to model stable crack growth and fracture of 2024-T3 aluminum alloy (bare and clad) panels for several thicknesses. The panels had either single or multiple-site damage (MSD) cracks subjected to uniaxial or biaxial loading. Analyses were also conducted on cracked stiffened panels with single or MSD cracks. The critical CTOA value for each thickness was determined by matching the failure load on a middle-crack tension specimen. Comparisons were made between the critical angles determined from the finite-element analyses and those measured with photographic methods. Predicted load-against-crack extension and failure loads for panels under biaxial loading, panels with MSD cracks, and panels with various number of stiffeners were compared with test data, whenever possible. The predicted results agreed well with the test data even for large-scale plastic deformations. The analyses were also able to predict stable tearing behavior of a large lead crack in the presence of MSD cracks. The analyses were then used to study the influence of stiffeners on residual strength in the presence of widespread fatigue cracking. Small MSD cracks were found to greatly reduce the residual strength for large lead cracks even for stiffened panels.

INTRODUCTION

Aging of the commercial transport fleets around the world increases the possibility of a reduction or loss of structural integrity through fatigue cracking. Widespread fatigue damage (cracks developing at several adjacent locations) is of great concern because the residual strength of a stiffened structure with a single long crack may be significantly reduced by the existence of adjacent smaller cracks as postulated by Swift [1]. Whereas a single long crack in a fuselage structure may produce flapping, a process by which a cracked fuselage would peel open in a small local region and lead to safe decompression, a fuselage with a long lead crack and multiple-site or multiple-element damage (MSD or MED) cracking may not flap. Tests on panels with long lead cracks and MSD are showing that residual strengths are strongly degraded [2]. Current fuselage designs must rely upon periodic inspections to assure safe operation [3]. One of the objectives in the

NASA Aging Aircraft Research Program [4] is to develop the methodology to predict flapping or failure in damaged fuselage structures in the presence of MSD or MED. The approach is to use a finite-element shell code with global-local, adaptive mesh capabilities and appropriate local fracture criteria to predict progressive failure in complex structures. In the future, fuselage structures may be designed by analysis, and verified by tests, to produce flapping or improved crack arresting capability under MSD or MED conditions.

Stable crack growth in metallic materials have been studied extensively using elastic-plastic finite-element methods [5-15]. These studies were conducted to develop efficient techniques to simulate crack extension and to examine various local and global fracture criteria. These criteria included crack-tip stress or strain, crack-tip-opening displacement or angle, crack-tip force, energy release rates, J-integral, and the tearing modulus. Of these, the crack-tip-opening angle (CTOA) or displacement (CTOD) was shown to be the most suited for modeling stable crack growth and instability during the fracture process. deKoning [7] showed that CTOA was nearly constant from initiation in an aluminum alloy. Shih et al [10] and Kanninen et al [11], in fracture analyses of both steel and aluminum alloys, showed that CTOA at initiation was much larger than the value needed for stable crack growth. Newman [12] used critical CTOD (or CTOA) values obtained from compact specimens to predict failure loads for several other crack configurations (two aluminum alloys and a very ductile steel) within 10 percent. Brocks and Yuan [13], Newman et al [14], and Demofonti and Rizzi [15] found that CTOD or CTOA was nearly constant after a small amount of crack growth for various materials and thicknesses. In some cases, the region of stable tearing where CTOD or CTOA was not constant appeared to be related to thickness but this region has not been defined quantitatively and its sensitivity to numerical calculations needs to be studied further.

Numerous investigators have also experimentally measured CTOA or CTOD during fracture. Luxmoore et al [16] showed that CTOA was constant from the onset of stable crack growth in two aluminum alloys, but found different values for different configurations. Paleebut [17], using a laser-interferometric displacement technique, measured CTOD (δ_i) at the initiation of stable tearing in compact specimens made of two aluminum alloys; these results agreed well with numerical values that Newman [12] used to model initiation, stable tearing and instability. Reuter et al [18], using microtopography [19], measured CTOD at the initial crack-front location and found a nearly linear relationship with crack extension for low-strength steel. These results would imply that CTOA was nearly constant from initiation for some materials. Newman et al [20] and Dawicke et al [21,22], using a high-resolution camera with a video system, have measured the critical angles during stable crack growth in aluminum alloys. These results also indicate that CTOA was constant after a small

amount of tearing (greater than the sheet thickness) for several crack configurations. The non-constant CTOA region, measured at the free surface, was shown to be associated with severe tunneling during the initiation of stable tearing.

To develop the fracture methodology to predict the influence of widespread fatigue cracking on fuselage structures, the behavior of multiple cracks in thin-sheet materials subjected to biaxial loading with various stiffener conditions, typical of fuselage structure, must be tested and analyzed. Recent tests, sponsored by the U.S. Federal Aviation Administration (FAA) Technical Center, were conducted by Broek et al [23] and deWit et al [24] on flat panels made of 2024-T3 aluminum alloy sheet with a wide variety of MSD crack configurations. These tests provided a large database on the effects of MSD cracking on residual strength. Newman et al [25], using the elastic-plastic finite-element analysis, has demonstrated that the CTOA criterion can accurately model the stable tearing behavior of multiple cracks. Donne and Doker [26], recently, conducted fracture test on 2024-T3 cruciform specimens subjected to biaxial loading. Many years ago, Leybold [27] and Vlieger [28] conducted fracture tests on 2024-T3 sheet panels with either 2024 or 7075 aluminum alloy stiffeners (intact or broken). These types of tests form the framework for establishing the creditability of the CTOA fracture criterion for predicting stable tearing and fracture of complex structure.

The objective of the present paper was to use the critical CTOA fracture criterion to study stable tearing and failure of 2024-T3 aluminum alloy panels (bare and clad) under a wide variety of loading conditions. Analyses were conducted on panels with single cracks under either uniaxial or biaxial loading, panels with multiple-site damage (MSD) cracking, and cracked stiffened panels. A two-dimensional, elastic-plastic (incremental flow theory, small strain), finite-element analysis (FEA) was used to model the fracture process. The critical CTOA value for each material thickness was determined by matching the failure load on a middle-crack tension specimen. Comparisons were then made between measured and predicted load-against-crack extension and failure loads for panels under biaxial loading, panels with MSD cracks, and panels with various number of stiffeners. The analyses were then used to study the influence of stiffeners on residual strength in the presence of widespread fatigue cracking.

NOMENCLATURE

A_c Cross-sectional area of crack or notch, mm^2
A_s Cross-sectional area of stiffener, mm^2
B Specimen thickness, mm
c Crack length (see Fig. 1), mm
c_i Initial crack length, mm
D Rivet diameter, mm
d Minimum element size along crack line, mm
d_r Spacing between multiple cracks, mm
E Young's modulus, MPa
L Total length of all cracks, mm
L_c Initial length of lead crack, mm
L_r Length of each small MSD crack, mm
P Applied load, kN
p Rivet pitch, mm
S Applied stress, MPa
S_k Peak stress during crack linkup (k = 1 to 3), MPa
S_n Net-section stress, MPa
S_f Gross failure stress, MPa
W Specimen width, mm
W_s Stringer width, mm
β Biaxial load or stress ratio
Δc Crack extension, mm
δ_i Critical sawcut displacement at initiation of crack, mm
λ Stiffener ratio defined by A_s/A_c
μ Stiffener ratio defined by A_s to total panel cross-sectional area
σ_{ys} Uniaxial yield stress (0.2% offset), MPa
σ_u Uniaxial tensile strength, MPa
ψ_c Critical crack-tip-opening angle, degrees

MATERIALS AND CRACK CONFIGURATIONS

Several 2024-T3 aluminum alloy material thicknesses were analyzed. Four materials were the bare alloy (1 to 6 mm-thick) and the other materials were the clad alloy (1 or 2 mm-thick). These materials are summarized in Table 1. For all material thicknesses, middle-crack tension specimen test results, with either sawcuts or cracks (see Fig. 1), were used to determine the fracture parameters to simulate sawcuts (δ_i) and cracks (ψ_c) in the finite-element analysis. Guide plates

were used to help prevent buckling in all tests.

Tests on the 2.3-mm thick bare alloy were conducted at NASA Langley on three specimen types: middle-crack tension M(T), compact tension C(T), and three-hole-crack tension (THCT) specimens, as shown in Figure 1. The M(T) specimens were 76 and 305 mm-wide, the C(T) specimens were 152.4 mm-wide, and the THCT specimens were 305 mm-wide. All specimens were fatigue precracked at a low stress level to produce a sharp fatigue crack. The THCT specimen simulates a crack growing in a stiffened panel, in that, the stress-intensity factor solution [12] is quite similar. Test results are reported in references 20-22.

Fracture tests were conducted by Broek et al [23] and deWit et al [24] on M(T) and multiple-site damage (MSD) specimens made of the 1 mm-thick clad and bare alloy, respectively. A typical MSD specimen is shown in Figure 2. The clad specimens were 508 mm-wide and the bare specimens were 2300 mm-wide. In both test programs, sawcuts were used instead of fatigue cracks. The MSD specimens contained a large lead sawcut (such as Sawcut #3) and anywhere from 2 to 20 MSD sawcuts.

Donne and Doker [26] conducted fracture tests on M(T) and cruciform (biaxial) specimens made of 6 mm-thick material. The M(T) specimen was 250 mm-wide and the biaxial specimens were 300 mm-wide in the test section. The biaxial specimen is shown in Figure 3. Both specimen types had fatigue cracks.

Leybold [27] and Vlieger [28] conducted fracture tests on 2024-T3 sheet panels with either 2024 or 7075 aluminum alloy stiffeners. The stiffened panel tests by Leybold had a single intact 2024 stringer, as shown in Figure 4(a). The stiffener width, W_S, and thickness was varied to give a stiffness ratio (λ) of 0.2 or 1. The stiffness ratio was defined as the ratio of stringer cross-sectional area to notch area. The panels had a very sharp notch of various lengths. The tests by Vlieger [28] had a central sawcut in a sheet with five 7075 stringers with the central stringer broken, as shown in Figure 4(b). In both test programs, the specimen widths were about 300 mm.

FINITE-ELEMENT ANALYSIS OF STABLE TEARING

An elastic-plastic finite-element code, ZIP2D, was used in the current study [12,25,29]. The elastic-plastic analysis employed the initial-stress concept of Zienkiewicz et al [30] which is based on incremental flow theory and the small-strain assumption. A multi-linear representation of the uniaxial stress-strain curve for 2024-T3 (and 7075-T6 for stringers) was used in the analyses with the von Mises yield criterion.

The finite-element models for all crack configurations analyzed were composed of two-dimensional, constant-strain, triangular elements. All sawcuts and cracks were located along a straight line, defined as the X-axis (see Fig. 4a). Symmetry was employed whenever possible to reduce the number of degrees-of-freedom. The minimum element size (d) along the line of crack extension was about 0.5 mm. This value has been found to be adequate for analyzing stable tearing in a wide variety of materials, as shown by Newman [12]. Equal-lateral triangles were used along the crack line so that cracks moving in either the positive or negative X-direction, such as in MSD crack configurations, would experience the same local mesh pattern. This pattern was found to be necessary to maintain nearly symmetric crack extension for the MSD crack configurations. Fictitious springs were used to fix displacement boundary conditions along the X-axis and to change boundary conditions associated with crack extension. For free nodes along the crack line, the spring stiffness were set equal to zero; for fixed nodes, the stiffness were assigned extremely large values. See reference 12 for details on the elastic-plastic finite-element analysis with crack extension and reference 25 for crack extension of multiple cracks.

In the FEA, a critical value of CTOA (ψ_c) was chosen as the fracture criterion for stably tearing cracks. Whenever the CTOA equaled or exceeded a preset critical value (ψ_c) during incremental loading, the crack-tip node was released and the crack advanced to the next node. This process was repeated until crack growth became unstable under load control or the crack reached the desired length under displacement control. The critical ψ_c value was selected by trial-and-error to match the average failure load measured on several M(T) specimens.

To simulate the effects of a sawcut, a critical sawcut displacement, δ_i , was selected to model the deformations that take place at a sawcut before a crack would initiate. Again, the critical value was selected to match the load require to initiate a crack at the sawcut. Once a crack had initiated, the critical angle was used to grow the crack. Table 1 gives a summary of the critical fracture parameters determined from various thickness 2024-T3 aluminum alloy M(T) specimens. These fracture parameters were used to predict stable crack extension and failure of the MSD crack configurations, the biaxially-loaded specimens, and the cracked stiffened panels.

CRITICAL CTOA MEASUREMENTS

Photographic techniques have been developed to measure critical CTOA values during crack initiation and stable tearing on several different types of laboratory specimens. In one method, a high-resolution optical microscope connected to a video system was used to record images of the deformed crack surfaces [21,22]. In each frame, the critical value of CTOA was measured at several locations behind the crack tip. For consistency, a standard distance from 0.5 to 1.5 mm was selected. In the second method, a digital-imaging correlation (DIC) method [31] was used to

record digitized images of speckle patterns around the crack-tip location. These two methods produced essentially the same CTOA values during stable tearing. A detailed description of these methods are given in Dawicke and Sutton [21].

Stable crack growth experiments were conducted on three specimen types: middle-crack tension M(T), compact tension C(T), and three-hole-crack tension (THCT) specimens, see Newman et al [20]. The standard laboratory specimens, M(T) and C(T), were selected to illustrate the influence of specimen type and loading on critical CTOA values. The THCT specimen was selected to measure CTOA in a structurally-configured specimen. The THCT specimen has a stress-intensity factor solution similar to a cracked stiffened panel [12]. The critical CTOA was measured during the fracture process on these three specimens. The results are shown in Figure 5. The critical angle ψ_c is plotted against crack extension, Δc. For each increment of crack extension, several values of ψ_c were measured and the average is plotted. The initial fatigue crack surfaces were flat and showed a small amount of tunneling in the interior. During the early stage of stable tearing, however, the crack front exhibited severe tunneling in the interior and the crack surfaces were still relatively flat [21,22]. The vertical line indicates the approximate location where the crack surfaces had completed the transition from flat to shear mode fracture (45 deg. slant through the thickness). The ψ_c values measured during crack initiation were high but dropped sharply during crack extensions equal to about the sheet thickness. Afterwards, the critical angle appeared to level off between 5 to 7 degrees. The solid horizontal line is the ψ_c value (6 degs.) determined from the FEA to fit the failure loads on several M(T) test specimens. Newman et al [20] and, later, Dawicke and Sutton [21] traced the reason for the high CTOA values during crack initiation to severe crack-front tunneling and the large plastic deformations on the specimen surface (recorded with the photographic methods).

DETERMINING CRITICAL CTOA FROM MIDDLE-CRACK TENSION SPECIMENS

The method used to determine the critical CTOA from a fracture test on a 6 mm-thick M(T) specimen is illustrated in Figure 6. The applied load is plotted against crack extension (measured by electrical potential [26]). From the FEA, using the full stress-strain curve of the material, a trial-and-error procedure was used to select a critical angle such that the analysis would match the test maximum load. The critical angle, ψ_c, was found to be 5 degrees assuming plane-stress conditions. Results from the FEA are shown by the solid curve. The analysis tended to overestimate crack extension in the early stages of crack growth. However, this is believed to have been caused by severe crack tunneling during crack initiation. Tunneling is expected to be nearly equal to the plate thickness. A comparison between the measured and predicted crack-opening displacements (COD) measured at the centerline of the M(T) specimen is shown in Figure 7. The predicted

displacements were in excellent agreement with the test results.

PREDICTING FAILURE OF MULTIPLE-SITE DAMAGE SPECIMENS

The critical CTOA (ψ_c) for cracks and δ_i for sawcuts determined from the M(T) specimens made of the 2024-T3 Alclad and bare materials were used to predict the stable crack growth behavior of the MSD panels tested by Broek et al [23] and deWit et al [24]. A crack-mouth-opening displacement gage was placed at the centerline of the large lead sawcut (like Sawcut #3 in Fig. 2) to record the load-displacement record during the tests. In general, the displacement record gave several peak stresses (S_k) during stable tearing and crack linkup, in addition to the maximum failure stress (S_f). Comparisons are made between measured and predicted peak stresses during crack linkup. In reference 24, videos were also taken of each test to record stable crack extension and crack linkup. Comparison are also made between measured and predicted crack initiation, crack extension, and failure loads on the panels.

A comparison of measured and predicted results for all of the MSD panels test by Broek et al [23] is given in reference 25. The results for only one of the panels will be shown here. The test had a large sawcut in the center with two smaller MSD sawcuts on either side of the large sawcut, like than shown in Figure 2. Figure 8 shows applied stress plotted against the total crack length, L, of all sawcuts and cracks. The tests results indicated three peak stresses S_1, S_2 and S_3. The maximum stress, S_f, corresponded to the second peak stress. These stresses are plotted as horizontal lines because they could not be related to any particular crack length. Predicted results are shown as the solid curve (δ_i = 0.075 mm; ψ_c = 5.1 degs.). The first and second peak stresses from the analysis were within 2 percent of the test results, while the final peak stress (S_3) was about 5 percent lower than the test result. Final failure with a single large crack corresponded to nearly net-section stress $S_n = \sigma_{ys}$ (dotted line). A comparison between the test and FEA results for the other panels demonstrated that the analysis with a critical CTOA could predict crack linkup and failure within about 5 percent.

The objective of the test program conducted by the National Institute of Standards and Technology (NIST) [24] was to study the fracture behavior of very large-scale, thin-sheet aluminum alloy specimens with MSD crack configurations. The test program consisted of ten fracture tests on 2300 mm-wide, 1 mm-thick, 2024-T3 aluminum alloy panels with a single large sawcut and 6 to 20 MSD sawcuts of various size and location. A summary of the panels tested is shown in Table 2. All but one of the panels were restrained from buckling.

At the beginning of the test program, the FEA method developed at NASA Langley was used to predict the load-crack-extension behavior of tests from MSD #2 to #10 based only on the results

from the first test (MSD #1). The only exception was test MSD #6 which was conducted without anti-buckling guides. In order to calibrate the finite-element analysis (before any CTOA measurements were made on the material), the critical CTOA was evaluated from test MSD #1. This panel was tested with a total sawcut of 355 mm. The load-crack-extension results from this tests was used to find the two fracture parameters (δ_i, ψ_c) that are required to simulate fracture of panels with sawcuts. The critical displacement at the sawcut tip was selected as 0.2 mm based on the crack-initiation load. The critical CTOA value was found to be 3.4 degrees. The calculated load-against-crack extension agreed well with the test results. These two parameters were used to predict the behavior of all other panels before the tests were conducted. These results were provided to NIST prior to the tests.

Again, the results for only one of the panels will be shown here. The test had a large sawcut in the center with six smaller MSD sawcuts on either side of the large sawcut. Figure 9 shows applied stress plotted against the length of the large lead crack as it grows and links up with the other sawcuts or cracks. The boxes at the bottom of the figure show a schematic of the tip of the lead sawcut and the placement of the three MSD sawcuts. The test results from the video camera are shown by the symbols. Again, the predicted results are shown as the solid curve (δ_i = 0.2 mm; ψ_c = 3.4 degs.). The predicted results agreed well with the test, especially the maximum failure load. To demonstrate the influence of sawcuts on crack linkup and failure, a prediction was also made with the sawcut parameter δ_i set to zero, as shown by the dashed curve. Although the maximum failure load was only slightly affected, the crack linkup behavior was greatly influenced, being 30 percent lower than the test with sawcuts. Table 2 gives a comparison between the maximum test loads and those predicted from the finite-element analyses. With the exception of test #5, all predictions were within about 6 percent of the test loads. The predicted results for loads at crack linkup also agreed reasonable well with the test results recorded on movie and video systems used by NIST.

During the test program, the photographic method [21] was used on several occasions to make measurement of the critical CTOA during stable tearing. The long-focal length, high resolution camera and video system was used to record the crack-surface profile during stable tearing. Material from the first test (MSD #1) was also provided to NASA to make CTOA measurements on small laboratory M(T) specimens (75 mm-wide). Several hundred measurements were made on the large and small specimens. After cracks had initiated from the sawcuts and grown for about one thickness, the critical CTOA value approached a constant of about 5.5 degrees. The CTOA values were basically the same for the small laboratory test specimens and the wide panel tests. This observation is crucial in the verification of the critical CTOA fracture

criterion.

The most striking difference between the CTOA values measured on the test specimens and that used in the analyses was the large difference between the angles. The average of the tests was 5.5 degrees and the computed value was 3.4 degrees. The large discrepancy is believed to be due to buckling of the panels above and below the anti-buckling guides. Observations of the test panels during fracture clearly showed severe buckling of the unrestrained panel. But further study is required to resolve the discrepancy.

PREDICTING FAILURE OF BIAXIALLY-LOADED SPECIMENS

Donne and Doker [26] conducted fracture tests on cruciform specimens made of 6 mm-thick material. The biaxial specimen with a fatigue crack is shown in Figure 3. Tests were conducted under displacement control for the load perpendicular to the crack and load control in the other direction to maintain a constant biaxial ratio (β). Guide plates were used in the tests with negative β.

A comparison between measured and predicted load-against-crack extension is shown in Figure 10. The applied load is plotted against crack extension (again measured by electrical potential [26]). The analyses were conducted under load control to maintain a constant β ratio. The predicted results (solid curves) tended to greatly overestimate crack extension in the early stages of crack growth, similar to that observed for the M(T) specimen. But here the discrepancies were much larger. The reason for the large differences is unknown but, again, they may be related to severe tunneling. A comparison between the measured and predicted crack-opening displacements (COD) measured at the centerline of the biaxial specimen is shown in Figure 11. The predicted displacements agreed well with the test results for all biaxial ratios. The analyses using the CTOA method was able to predict failure loads within 10 percent of the test loads for all biaxial ratios.

PREDICTING FAILURE OF CRACKED STIFFENED PANELS

To predict stable crack growth and failure of cracked stiffened panels, the finite-element method was used to model both the sheet and stiffeners, as shown in Figure 12. The stiffener model lies in the same plane as the sheet and is connected to the sheet at the rivet locations. Both the sheet and stringers are modeled with constant-strain elements and have multiple-linear stress-strain curves for the respective materials. The rivet connection was modeled by an elastic-perfectly plastic shear spring with an elastic modulus of 70,000 MPa, Poisson's ratio of 0.3, and a shear yield of 200 MPa. Because constant-strain elements were used to model the stringers, analyses were conducted on a simulated stringer with rivet loading, as shown in Figure 13. Mesh A (not shown)

had 826 elements modeling the stringer and rivet (rivet and sheet were tied together). Mesh B had 16 elements, as shown, and this type of mesh was used to model all stringers. Figure 14 shows a comparison between the rivet displacements calculated from Mesh A and B. As expected, Mesh B (dashed curves) was too stiff and gave smaller displacements than Mesh A for a given rivet load (solid curves). Altering the elastic modulus of the material for Mesh B (E' = 0.5E) gave elastic displacements that matched well with displacements from Mesh A. The yield properties of the materials were not changed. Thus, in the panel analyses, the elastic modulus of the stringer material was set to 0.5E.

Leybold [27] conducted fracture tests on 2024-T3 sheet panels with a single stiffener, as shown in Figure 4(a). The stiffener width, W_S, and thickness was varied to give a stiffness ratio (λ) of 0.2 or 1. The stiffness ratio was defined as the ratio of stringer cross-sectional area to notch area. The panels had a very sharp notch of various lengths. Figure 15 shows a comparison of measured and predicted failure stresses on panels with no stiffener [32] and those with $\lambda = 0.2$ and 1 [27]. The symbols show the test results and the curves show the predicted results using a critical angle of 6 degrees. The test results and predicted failure stresses agreed well.

Vlieger [28] conducted fracture tests on 2024-T3 sheet panels with multiple stiffeners. The tests had a central sawcut in a sheet with five 7075 stringers with the central stringer broken, as shown in Figure 4(b). Figure 16 shows a comparison of measured and predicted stable crack extension on panels with different initial sawcuts. The symbols show the test results and the curves show the predicted results using fracture parameters (δ_i, ψ_c) determined from M(T) specimen tests. Again, the test results and predictions agreed fairly well.

INFLUENCE OF MSD CRACKING ON BIAXIALLY-LOADED STIFFENED PANELS

Swift [1] had postulated that small MSD cracks may have a large influence on the residual strength for a large lead crack. This phenomenon has been demonstrated using the FEA and the critical CTOA fracture criterion on flat panels [25]. How stiffeners impact the influence of MSD cracks on lead-crack behavior needs to be studied. The FEA and the CTOA criterion was used to study this behavior for the 2024-T3 thin-sheet material ($\psi_c = 5.1$ deg.; $\delta_i = 0$). An MSD panel with seven 7075 stringers (central stringer broken), as shown in Figure 17, was analyzed. The finite-element model, shown in Figure 12, was used with symmetry conditions imposed along the X- and Y-axes. The panel had a lead crack ($L_c = 35$ cm) with various number of smaller MSD cracks placed at equal intervals (d_r) to simulate rivet spacing. The stiffness ratio, cross-sectional area of stringer to total cross-sectional area (μ), was either 0.15 or 0.3.

Figure 18 shows the predicted results for a single crack (dashed curve) and for a lead crack

with 15 MSD cracks (solid curve). This figure shows applied stress plotted against lead crack half-length and demonstrates that, even with typical stiffeners, a large number of MSD cracks can cause a large reduction in residual strength. Results shown in Figure 19 are for the identical crack configuration, as shown in Figure 18, except that the stiffener ratio was doubled to 0.3. The final results are quite similar. The increase in the stiffener ratio did not adversely change the influence of MSD on residual strength. The results for only three MSD cracks (located just in front of the lead crack) are also shown. The residual strength is only slightly lowered from the single crack behavior. These results demonstrate the sensitivity of lead-crack behavior with the number and location of MSD cracking.

A comparison between the relative residual strength ratio from test and analyses for various size MSD cracks are shown in Figure 20. This figure shows the ratio of residual strength with 15 MSD cracks to that with only a single lead crack plotted against MSD crack length. The test results (symbols) were obtained from Goranson [33] for flat sheets (no load transfer) and lap-splice joints (load transfer) with MSD at the rivet locations. The rivet diameter was about 5 mm. (There were no stringers in the tests conducted in reference 33.) The curves were calculated results for a flat panel and panels with seven stringers for $\mu = 0.15$ or 0.3 for various size MSD cracks. For the larger MSD crack sizes, the test and analyses agreed fairly well. However, the results for the smaller MSD cracks did not agree, presumably because rivet holes were not modeled in the analysis. Further testing and analyses, with damaged curved panels with rivets and stringers, are necessary to substantiate the use of the FEA and the critical CTOA fracture criterion for lap-splice joints and buildup structure.

CONCLUSIONS

(1) Critical crack-tip-opening angle (CTOA) is independent of crack configuration and loading for 1 to 6 mm-thick 2024-T3 aluminum alloy material after a small amount of crack extension.

(2) Finite-element fracture simulations using the critical CTOA gives very accurate details of plastic deformation and stable tearing of cracks under complex loading, such as biaxial loading and stiffened panels.

(3) Finite-element analyses predict a significant influence of multiple-site damage (MSD) cracks on lead-crack behavior for both unstiffened and stiffened panels.

(4) Influence of MSD on lead-crack behavior in stiffened panels under biaxial loading is only slightly improved with larger stiffeners.

REFERENCES

[1] Swift, T., "Damage Tolerance in Pressurized Fuselages", New Materials and Fatigue Resistant Aircraft Design, 14th Symposium of the International Committee on Aeronautical Fatigue, June 1987.

[2] Maclin, J., "Performance of Fuselage Pressure Structure", 1991 International Conference on Aging Aircraft and Structural Airworthiness, C. E. Harris, ed., NASA CP-3160, Washington, D.C., 1992, pp. 67-75.

[3] McGuire, J. F. and Goranson, U. G., "Structural Integrity of Future Aging Airplanes", 1991 International Conference on Aging Aircraft and Structural Airworthiness, C. E. Harris, ed., NASA CP-3160, Washington, D.C., 1992, pp. 33-48.

[4] Harris, C. E., "NASA Aircraft Structural Integrity Program", NASA TM 102637, April 1990.

[5] Kobayashi, A. S.; Chiu, S. T. and Beeuwkes, R., "A Numerical and Experimental Investigation on the Use of the J-Integral", Engineering Fracture Mechanics, Vol. 5, No. 2, 1973, pp. 293-305.

[6] Anderson, H., "A Finite-Element Representation of Stable Crack Growth," Journal Mechanics and Physics of Solids", Vol. 21, 1973, pp. 337-356.

[7] de Koning, A. U., "A Contribution to the Analysis of Slow Stable Crack Growth", National Aerospace Laboratory Report NLR MP 75035U, 1975.

[8] Light, M. F.; Luxmoore, A. and Evans, W. T., "Prediction of Slow Crack Growth by a Finite Element Method", International Journal of Fatigue, Vol. 11, 1975, pp. 1045-1046.

[9] Rousselier, G., "A Numerical Approach for Stable-Crack-Growth and Fracture Criteria", Fourth International Conference on Fracture, Waterloo, Canada, Vol. 3, 1977, pp. 1-6.

[10] Shih, C. F.; de Lorenzi, H. G. and Andrews, W. R., "Studies on Crack Initiation and Stable Crack Growth", ASTM STP 668, 1979, pp. 65-120.

[11] Kanninen, M. F.; Rybicki, E. F.; Stonesifer, R. B.; Broek, D.; Rosenfield, A. R. and Nalin, G. T., "Elastic-Plastic Fracture Mechanics for Two-Dimensional Stable Crack Growth and Instability Problems", ASTM STP 668, 1979, pp. 121-150.

[12] Newman, J. C., Jr., "An Elastic-Plastic Finite Element Analysis of Crack Initiation, Stable Crack Growth and Instability", ASTM STP 833, 1984, pp. 93-117.

[13] Brocks, W. and Yuan, H., "Numerical Studies on Stable Crack Growth", ESIS Publicaton 9, 1991, pp. 19-33.

[14] Newman, J. C., Jr.; Shivakumar, K. N. and McCabe, D. E., "Finite Element Fracture Simulation of A533B Steel Sheet Specimens", ESIS Publication 9, 1991, pp. 117-126.

[15] Demofonti, G. and Rizzi, L., "Experimental Evaluation of CTOA in Controlling Unstable Ductile Fracture Propagation", ESIS Publication 9, 1991, pp. 693-703.

[16] Light, M. F.; Luxmoore, A. and Evans, W. T., "Prediction of Slow Crack Growth by a Finite Element Method", International Journal of Fatigue, Vol. 11, 1975, pp. 1045-1046.

[17] Paleebut, S., "CTOD and COD Measurements on Compact Specimens of Different Thicknesses", M.S. Thesis, Michigan State University, 1978.

[18] Reuter, W. G.; Graham, S. M.; Lloyd, W. R. and Williamson, R. L., "Ability of Using Experimental Measurements of w to Predict Crack Initiation for Structural Components", ESIS Publication 9, 1991, pp. 175-188.

[19] Kobayashi, T.; Irwin, G. R. and Zhang, X. J., "Topographic Examination of Fracture Surfaces in Fibrous-Cleavage Transition Behavior", ASTM STP 827, 1989, pp. 234-251.

[20] Newman, J. C., Jr.; Dawicke, D. S. and Bigelow, C. A., "Finite-Element Analyses and Fracture Simulation in Thin-Sheet Aluminum Alloy", Proceedings of the International Workshop on Structural Integrity of Aging Airplanes, Atlanta, GA, March 1992, pp. 167-186.

[21] Dawicke, D. S. and Sutton, M. A., "Crack-Tip-Opening Angle Measurements and Crack Tunneling under Stable Tearing in Thin Sheet 2024-T3 Aluminum Alloy", submitted to Experimental Mechanics Journal, 1993.

[22] Dawicke, D. S.; Sutton, M. A.; Newman, J. C., Jr. and C. A. Bigelow, "Measurement and Analysis of Critical CTOA for Thin-Sheet Aluminum Alloy Materials", presented at 25th National Symposium on Fracture Mechanics, Lehigh University, June 1993.

[23] Broek, D.; Thomson, D. and Jeong, D. Y., "Testing and Analysis of Flat and Curved Panels with Multiple Cracks", NASA Conference Publication 3274, Part I, September 1994, pp. 85-98.

[24] deWit, R.; Fields, R. J.; Mordfin, L.; Low, S. R. and Harne, D., "Fracture Behavior of Large-Scale Thin-Sheet Aluminum Alloy," NASA Conference Publication 3274, Part II, September 1994, pp. 963-984.

[25] Newman, J. C., Jr.; Dawicke, D. S.; Sutton, M. A. and Bigelow, C. A., "A Fracture Criterion for Widespread Cracking in Thin-Sheet Aluminum Alloys", Durability and Structural Integrity of

Airframes, Vol. I, A. F. Blom, ed., 17th Symposium International Committee on Aeronautical Fatigue, June 9-11, 1993, Stockholm, Sweden, pp. 443-468.

[26] Donne, C. D. and Doker, H., "Biaxial Load Effects on Plane Stress J-Δa- and δ_i -Δa-Curves", Proceedings 10th European Conference on Fracture, Berlin, Germany, September 20-23, 1994, pp. 891-900.

[27] Leybold, H. A., "A Method for Predicting the Static Strength of a Stiffened Sheet containing a Sharp Central Notch", NASA TN D-1943, August 1963.

[28] Vlieger, H., "The Residual Strength Characteristics of Stiffened Panels containing Fatigue Cracks", Engineering Fracture Mechanics Journal, Vol. 5, 1973, pp. 447-477.

[29] Newman, J. C., Jr.: Finite-Element Analysis of Fatigue Crack Propagation--Including the Effects of Crack Closure, Ph.D. Thesis, VPI & State University, Blacksburg, VA, May 1974.

[30] Zienkiewicz, O. C.; Valliappan, S. and King, I. P., "Elasto-Plastic Solutions of Engineering Problems", International Journal of Numerical Methods in Engineering, Vol. 1, 1969, pp. 75-100.

[31] Sutton, M. A.; Bruck, H. A. and McNeill, S. R., "Determination of Deformations Using Digital Correlation with the Newton Raphson Method for Partial Differential Correction", Experimental Mechanics, Vol. 29, No. 3, 1989, pp. 261-267.

[32] Newman, J. C., Jr., "Fracture Analysis of Various Cracked Configurations in Sheet and Plate Materials", ASTM STP-605, 1976, pp. 104-123.

[33] Goranson, U. G., "Damage Tolerance - Facts and Fiction", Durability and Structural Integrity of Airframes, Vol. I, A. F. Blom, ed., 17th Symposium International Committee on Aeronautical Fatigue, Stockholm, Sweden, June 9-11, 1993, pp. 3-105.

Table 1.- Critical CTOA determined from 2024-T3 M(T) specimens using the FEA.

Condition	B, mm	δ_i, mm	ψ_c, degs.	Ref.
Alclad	1	0.075	5.1	23
Bare	1	0.2	3.4 (a)	24
Bare	1.6	0	6.0	27
Alclad	2	0.2	6.5	28
Bare	2.3	0	6.0	20-22
Bare	6	0	5.0	26

(a) Buckling may have occurred during test (measured ψ_c was 5.5 degs.).

Table 2.- Comparison of measured and predicted failure loads on NIST multiple-site damage (MSD) fracture tests.

MSD Panel (a)	Number of sawcuts	Test load, kN	Predicted load, kN	Percent error
1	1	342.5	341.6 (b)	-0.3
2	1	428.4	427.0	-0.3
3	1	288.7	291.8	1.1
4	7	307.4	298.0	-3.0
5	7	405.7	359.9	-11.3
7	11	214.4	221.5	3.3
8	21	211.3	225.1	6.5
9	21	352.3	332.7	-5.6
10 (c)	11	232.2	221.5	-4.6

(a) MSD #6 was tested without anti-buckling guides.

(b) Fitted to test (δ_i = 0.2 mm, ψ_c = 3.4 deg.).

(c) MSD #10 was a repeat of MSD #7.

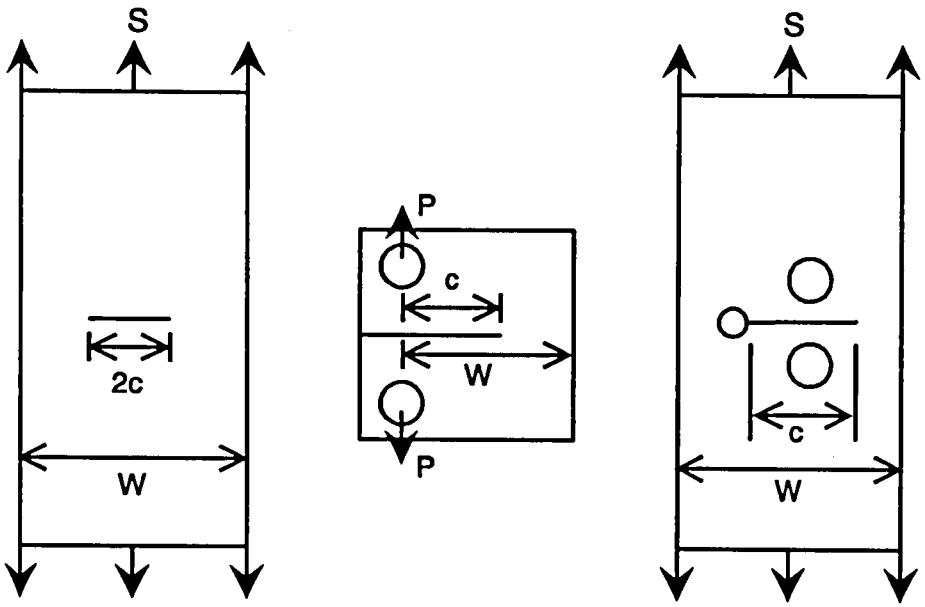

(a) Middle-crack tension (b) Compact tension (c) Three-hole-crack tension

Figure 1 - Laboratory fracture specimens tested and analyzed.

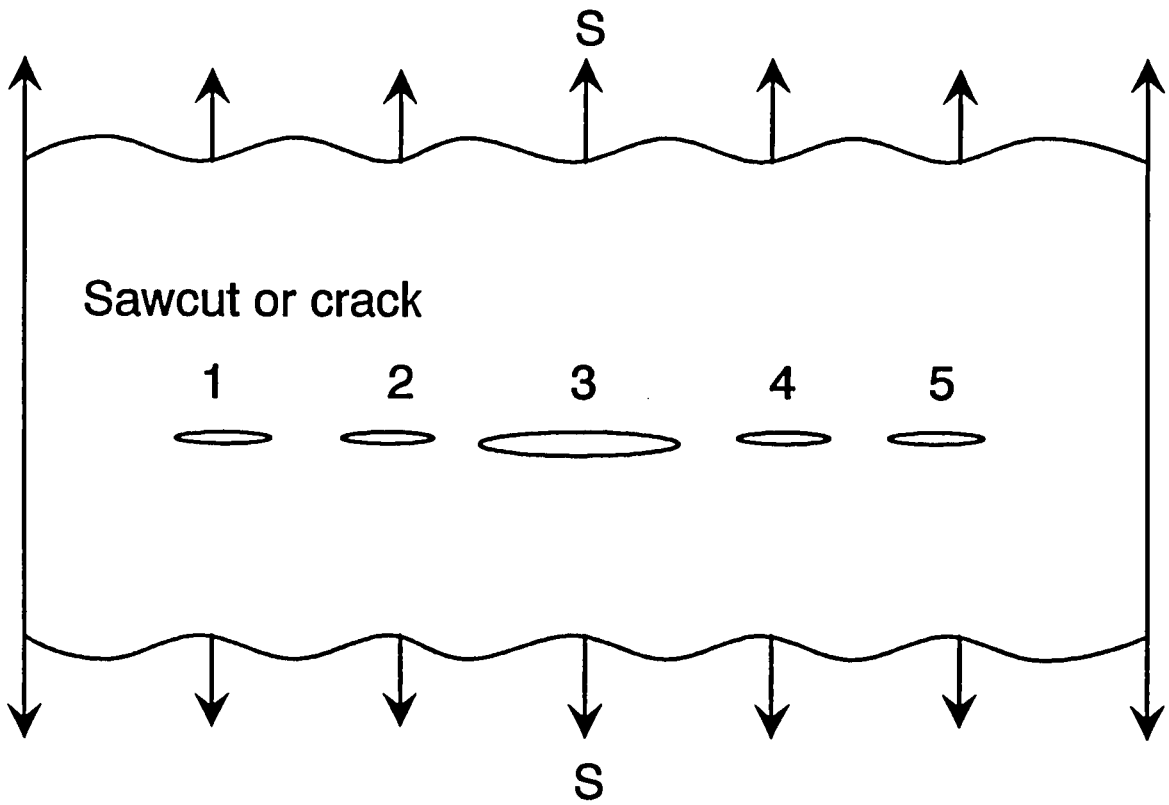

Figure 2 - Multiple-site damage (MSD) crack configuration..

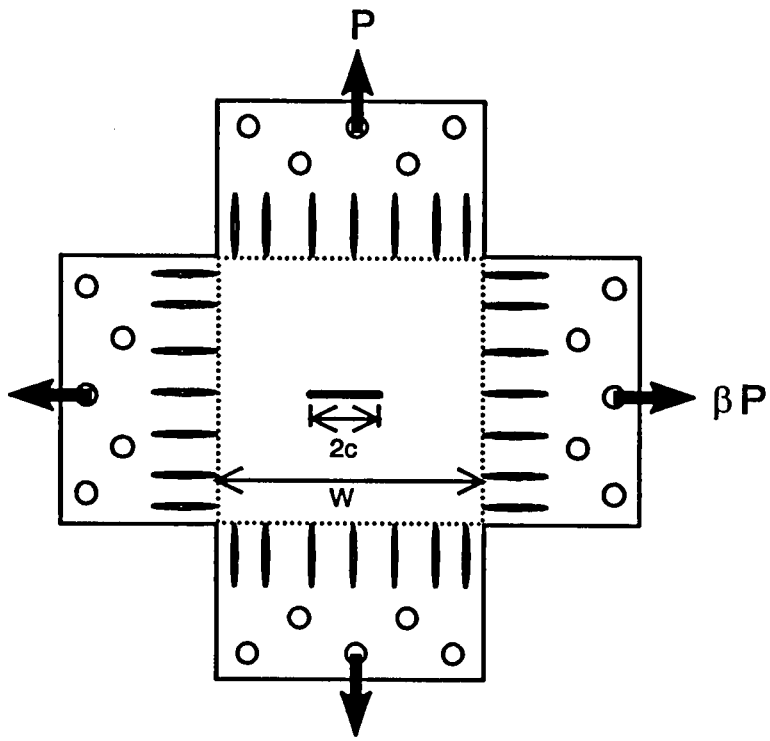

Figure 3 - Cracked panel subjected to biaxial loading.

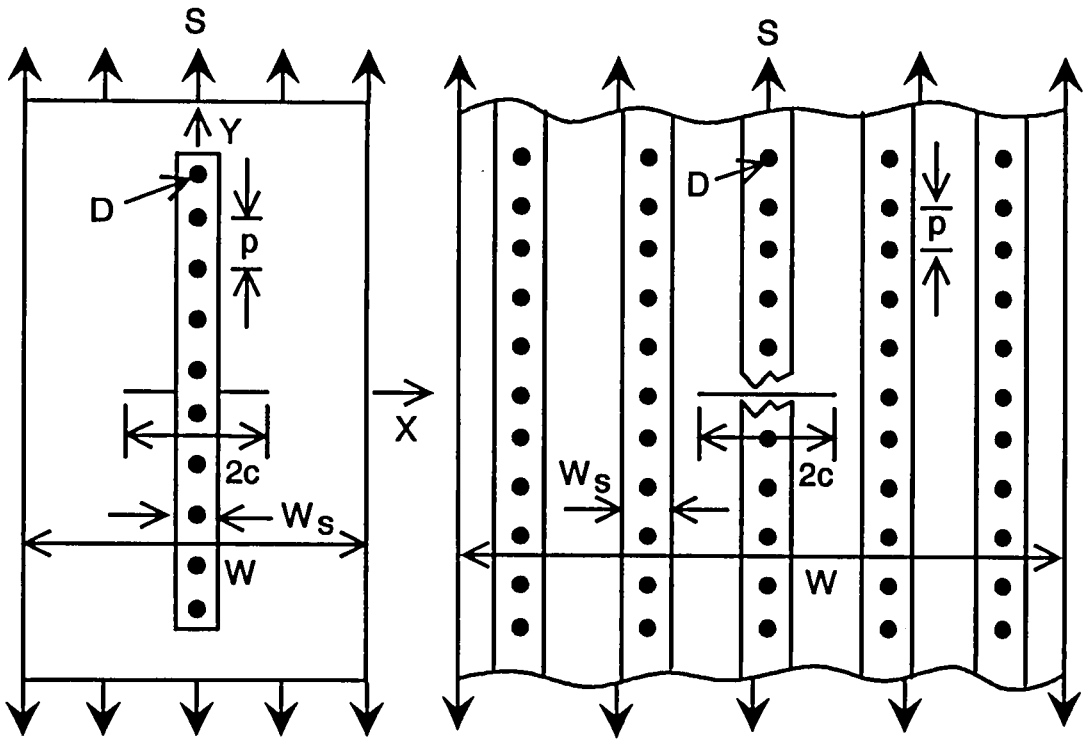

(a) Single stiffener panel.

(b) Multiple stiffener panel.

Figure 4 - Types of cracked stiffened panels analyzed.

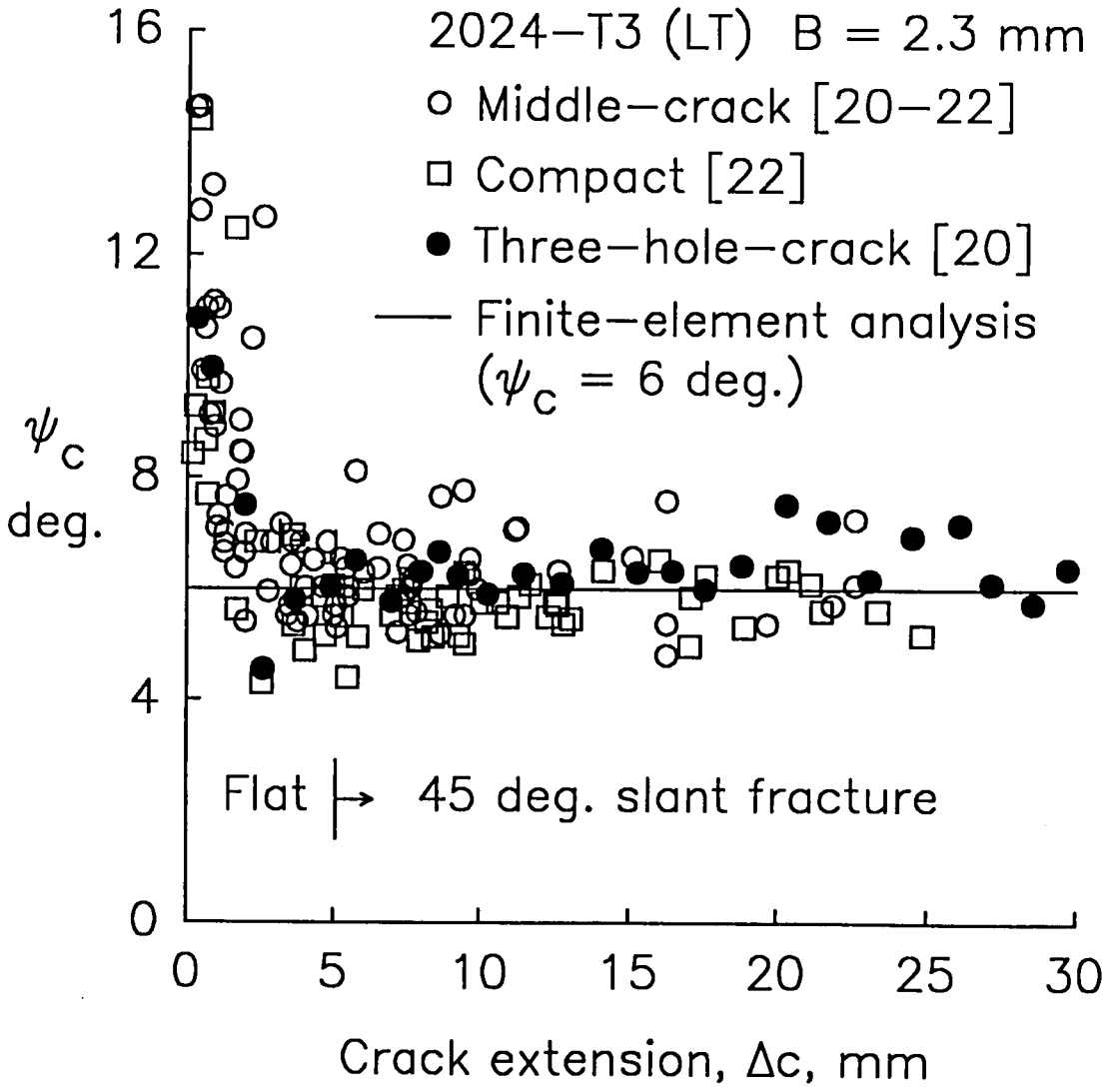

Figure 5 - Measured and calculated critical CTOA.

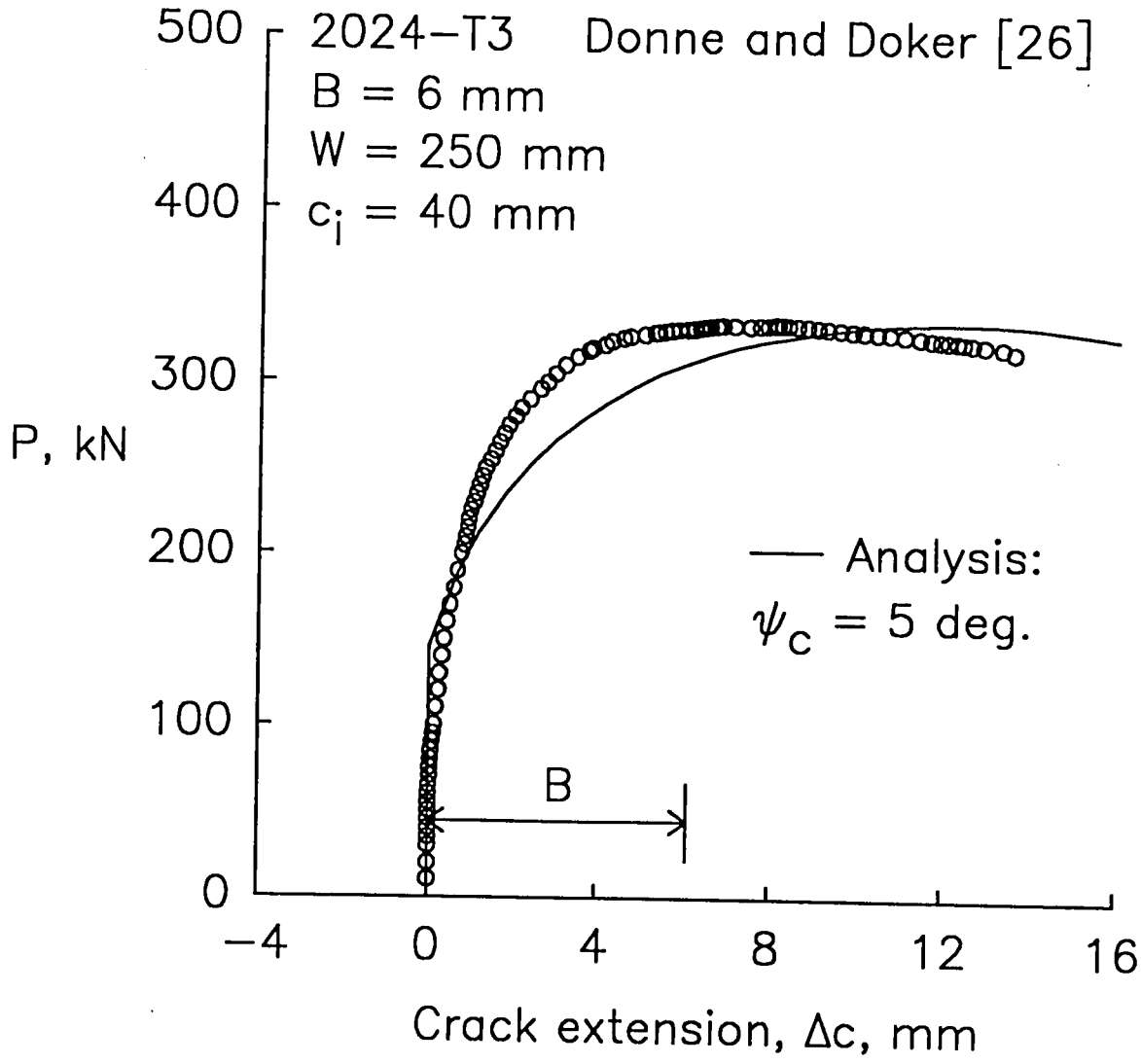

Figure 6 - Measured and calculated stable tearing for M(T) specimen.

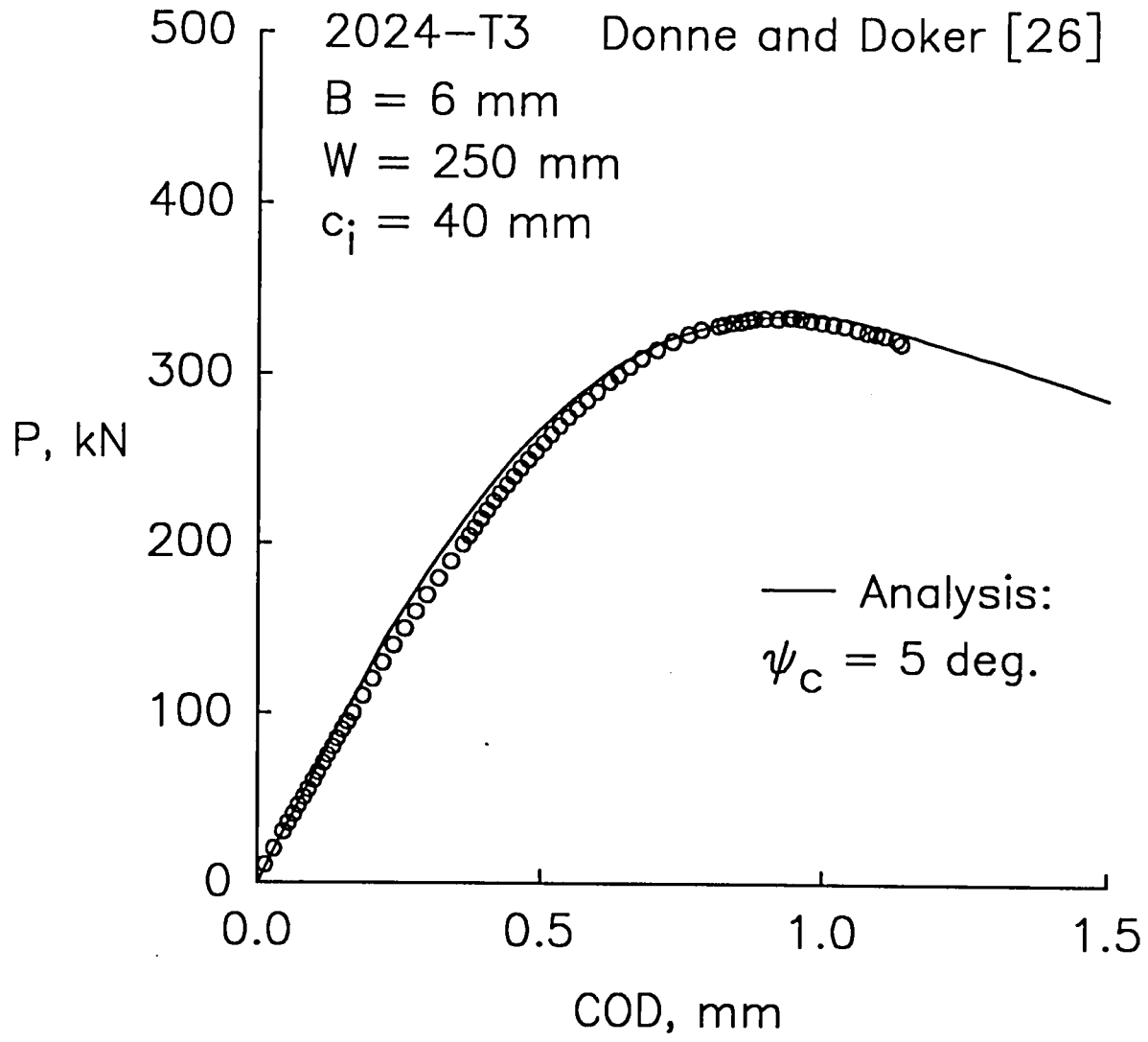

Figure 7 - Measured and calculated crack-opening displacements for M(T) specimen.

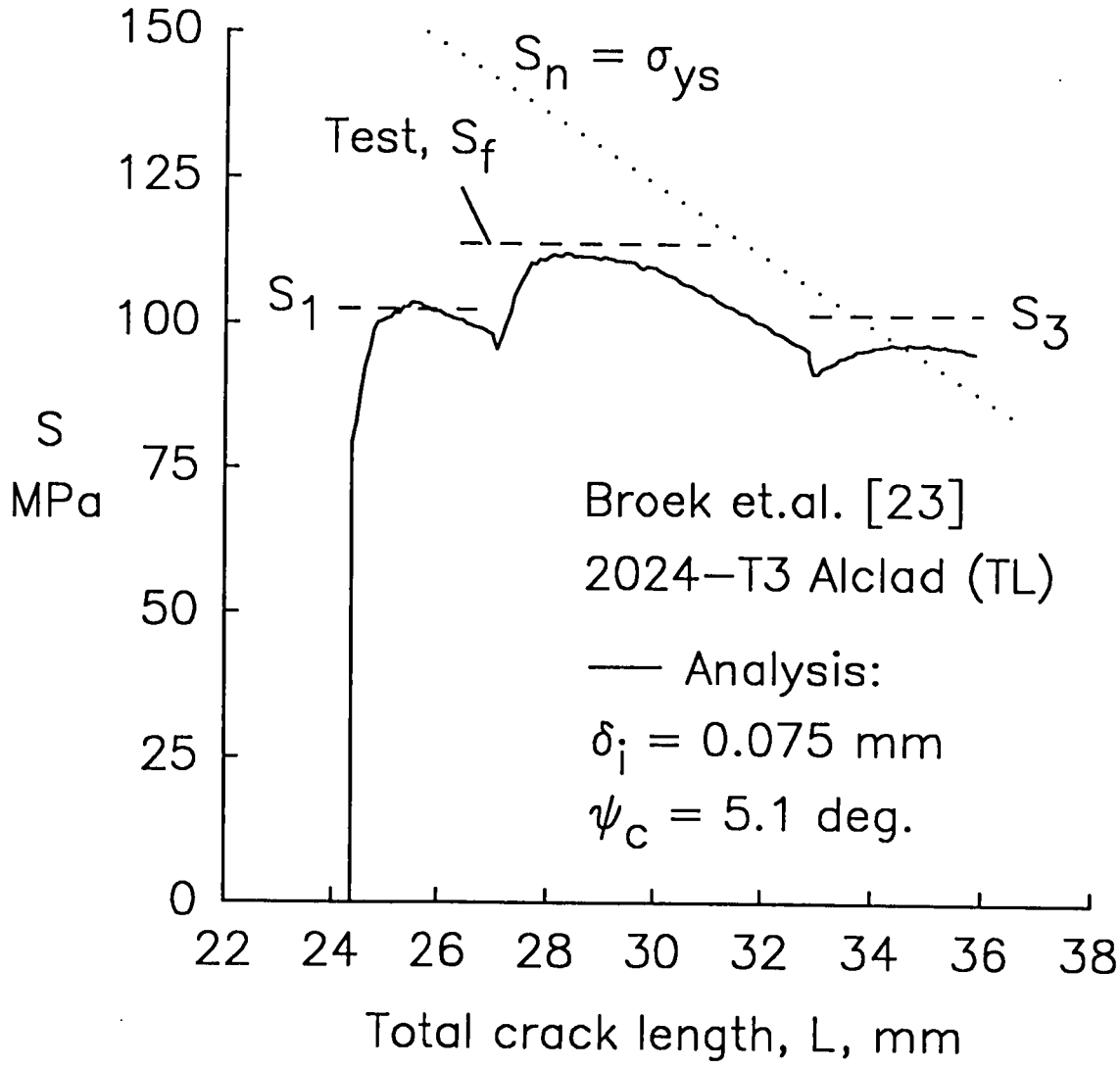

Figure 8 - Measured and predicted crack linkup and failure for specimen with five MSD cracks.

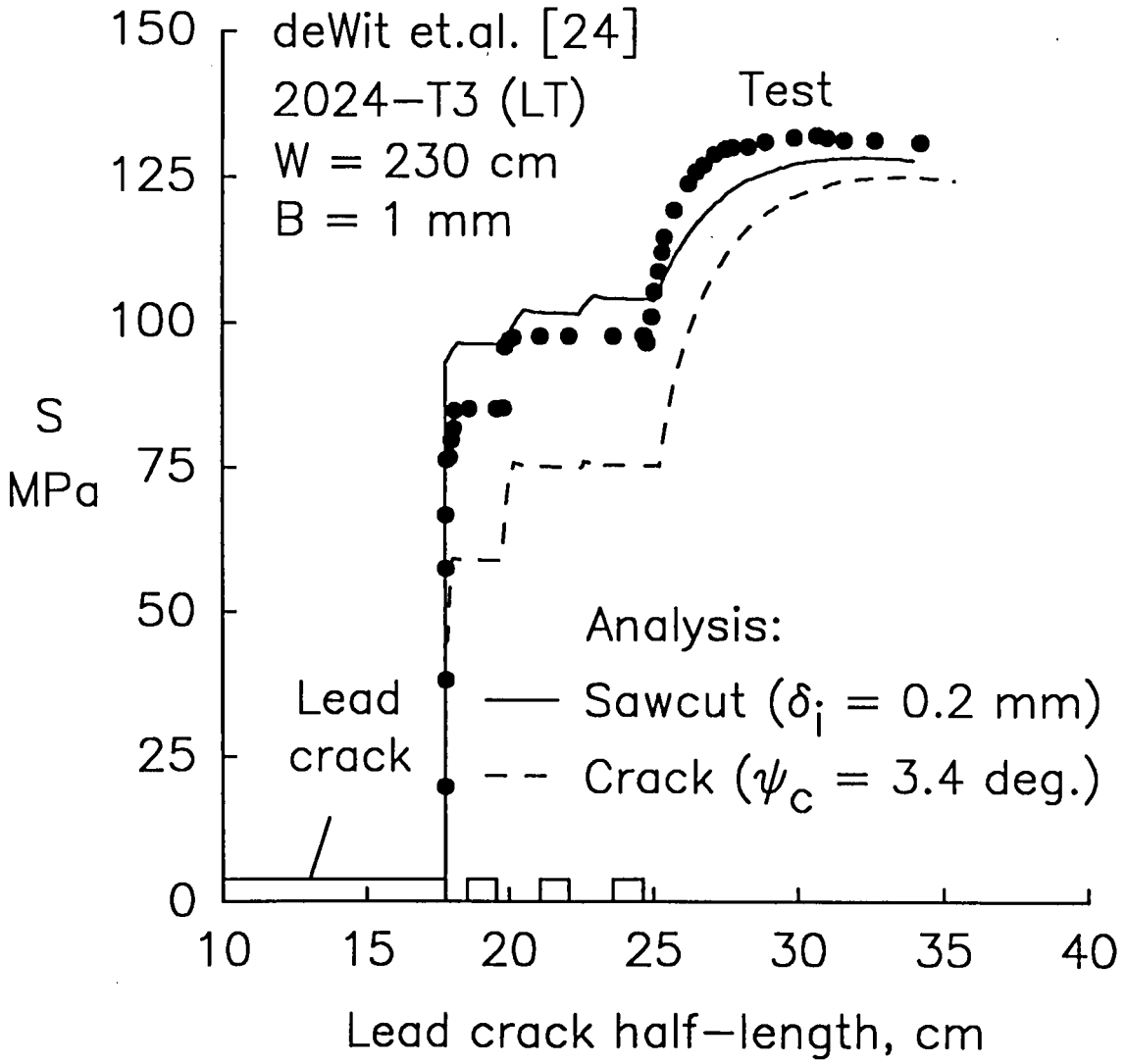

Figure 9 - Measured and predicted crack linkup and failure for large specimen with seven MSD cracks.

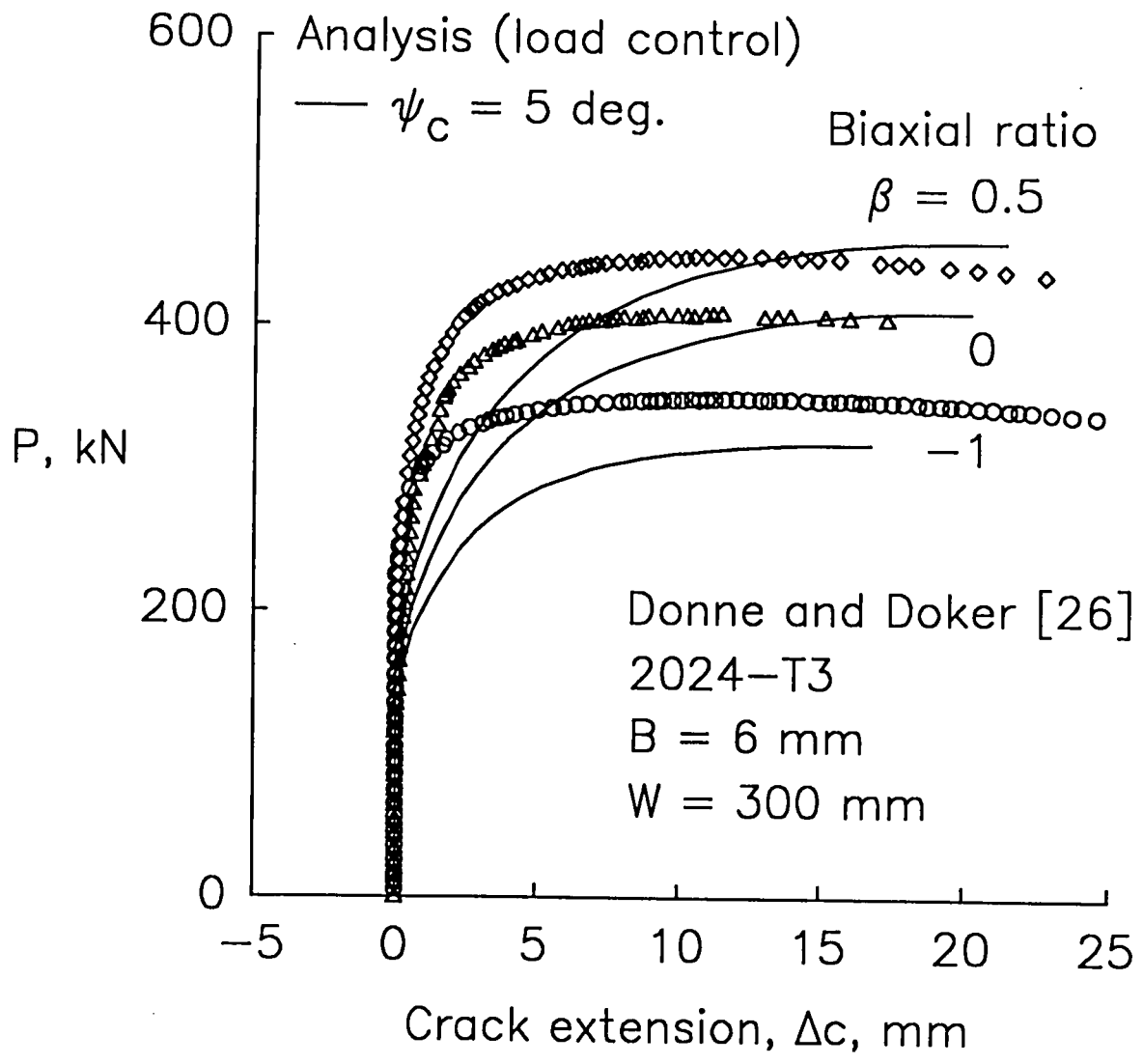

Figure 10 - Measured and predicted stable tearing for biaxial specimens.

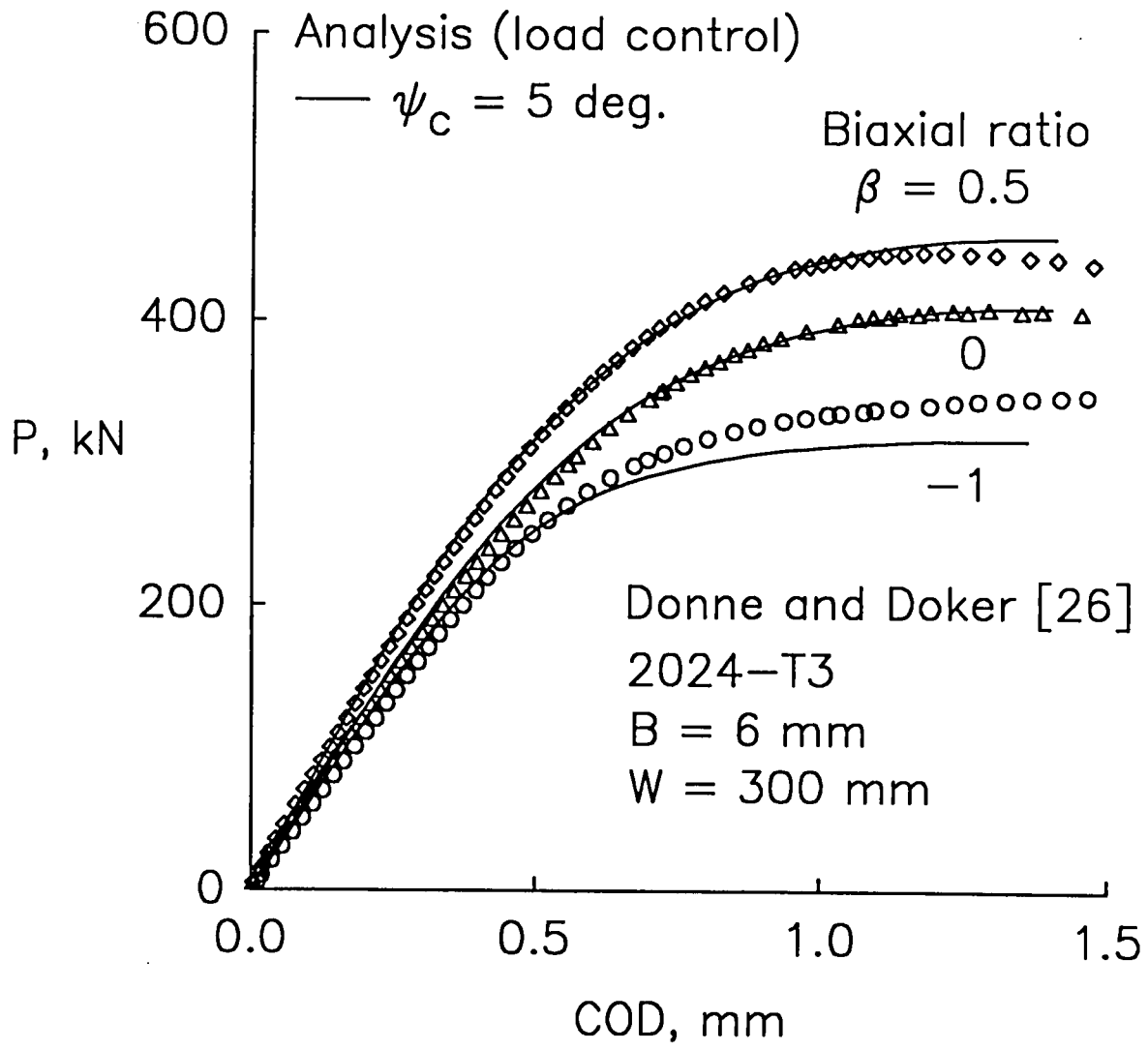

Figure 11 - Measured and predicted crack-opening displacements for biaxial specimens.

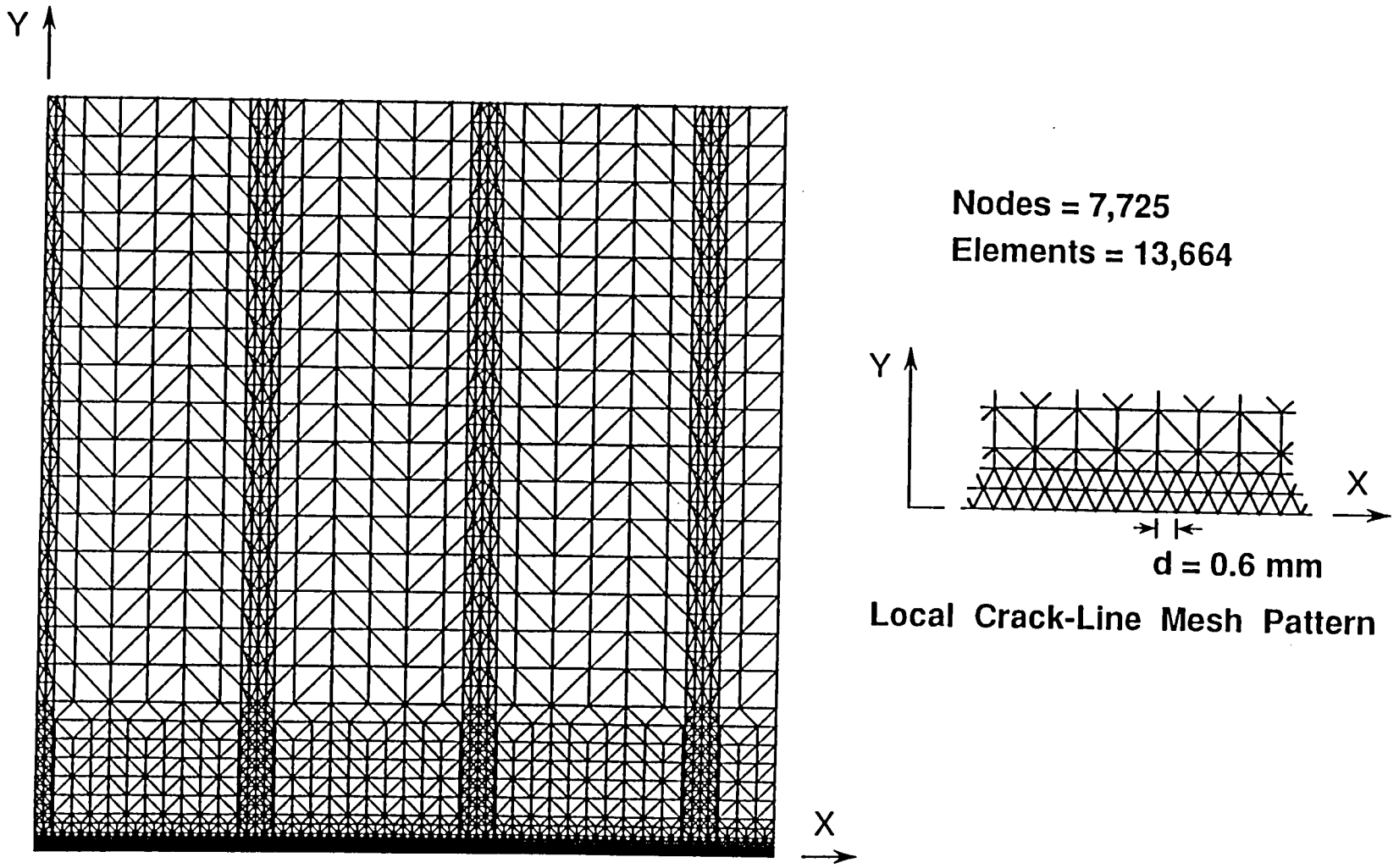

Figure 12 - Finite-element model of stiffened panel with MSD cracking.

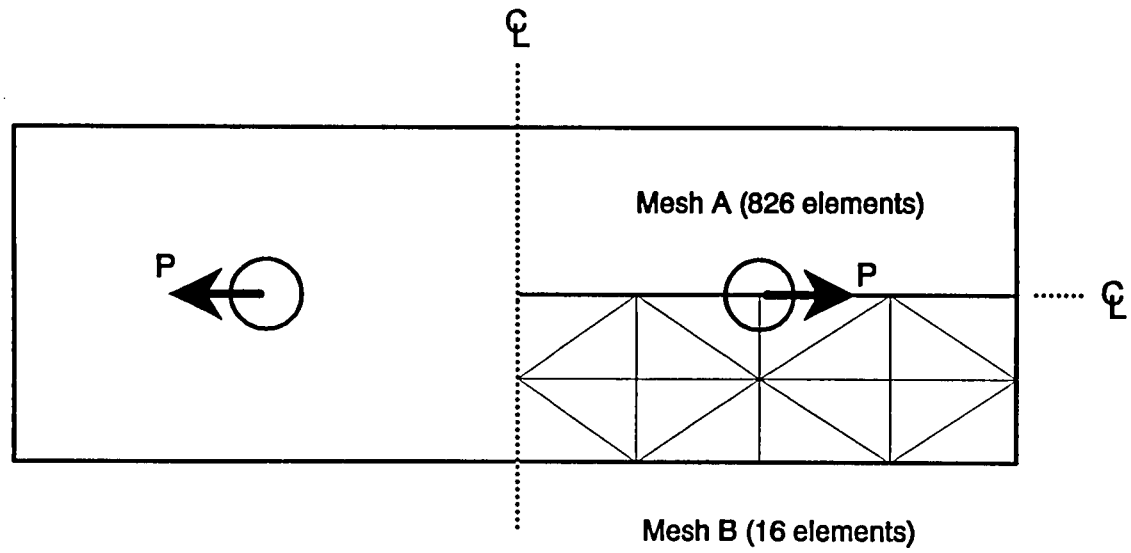

Figure 13 - Finite-element models for rivetted-loaded stringer.

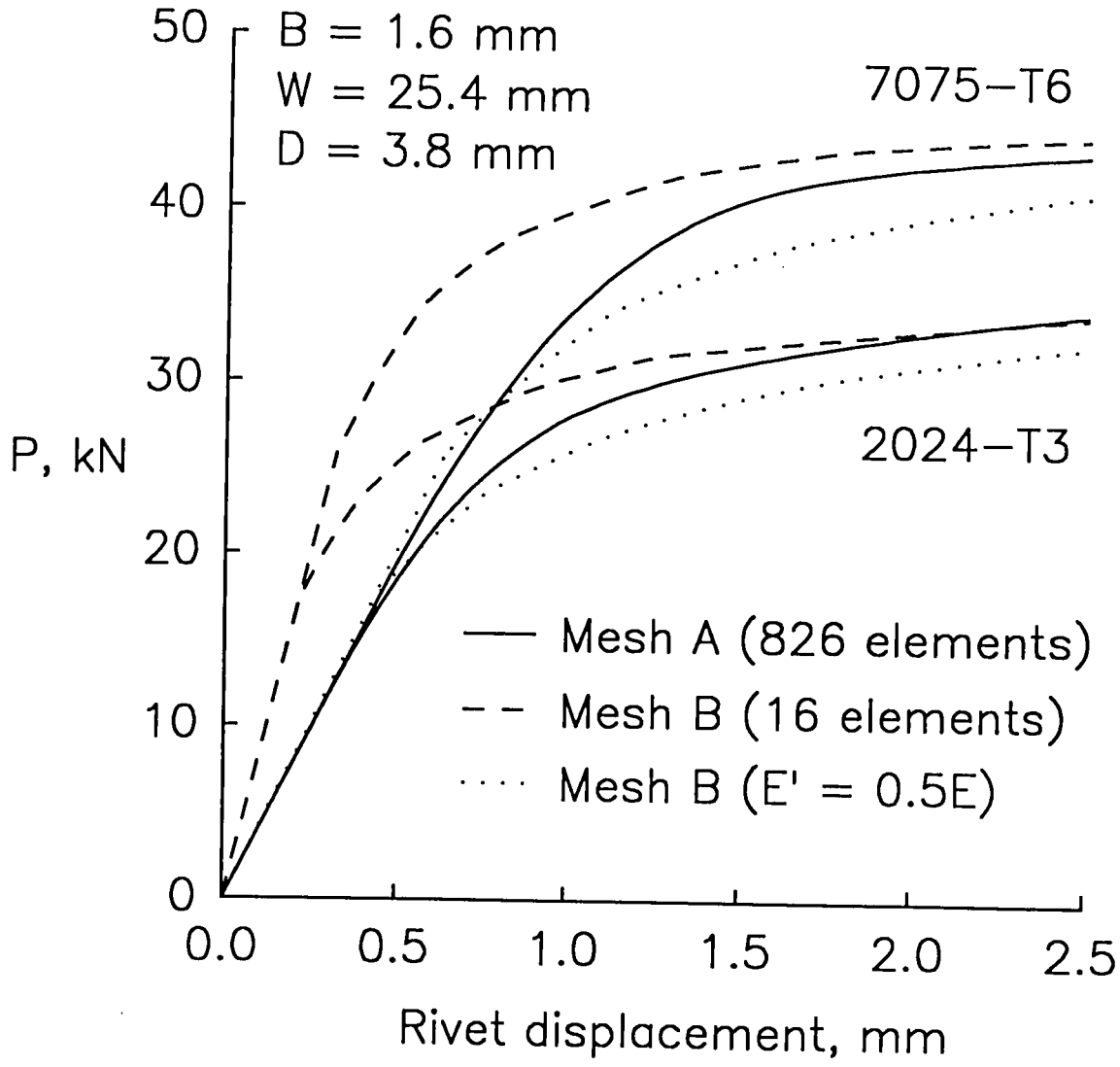

Figure 14 - Rivet displacements for various finite-element models of a stringer.

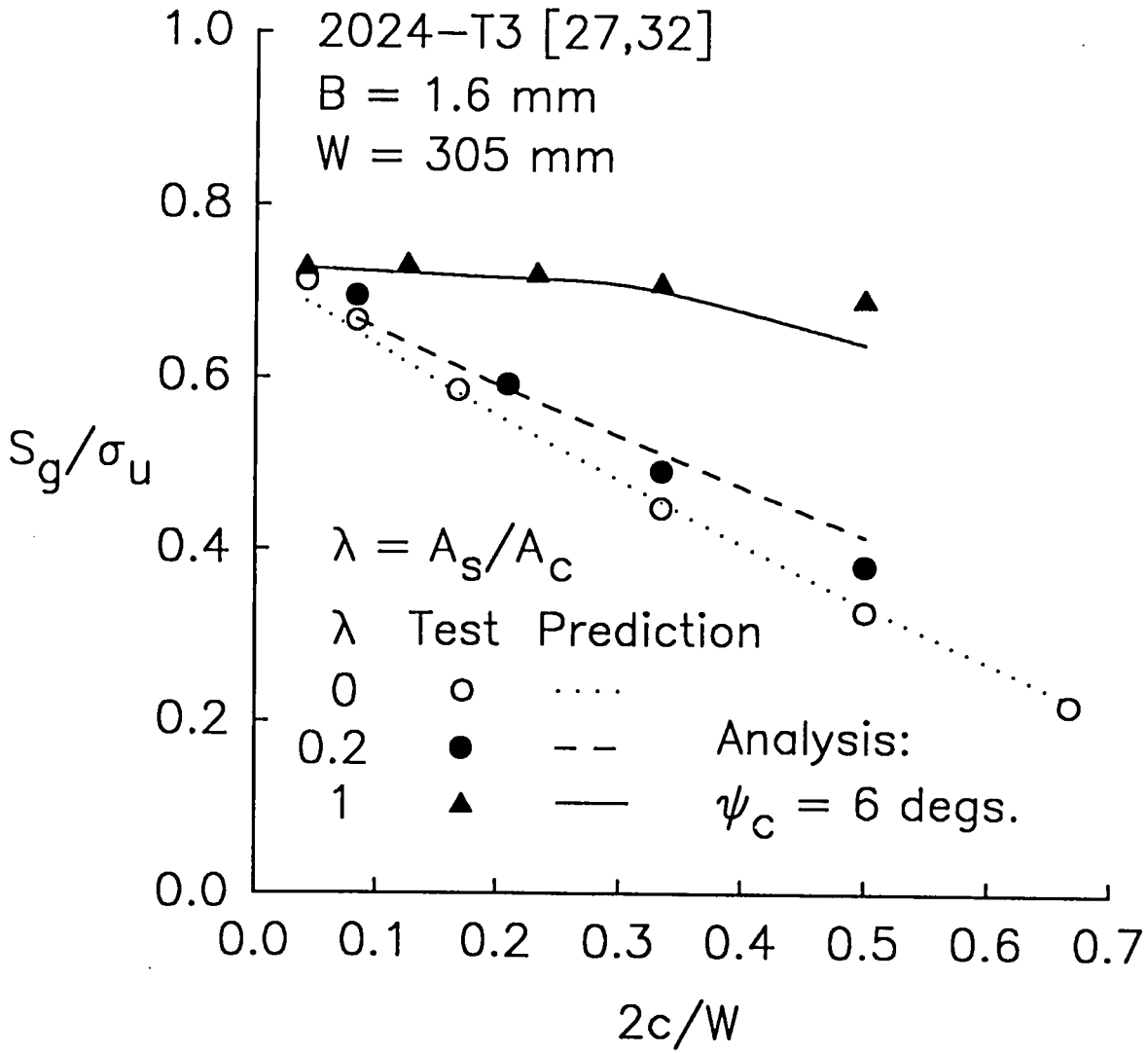

Figure 15 - Measured and predicted failure stresses for stiffened and unstiffened sheets.

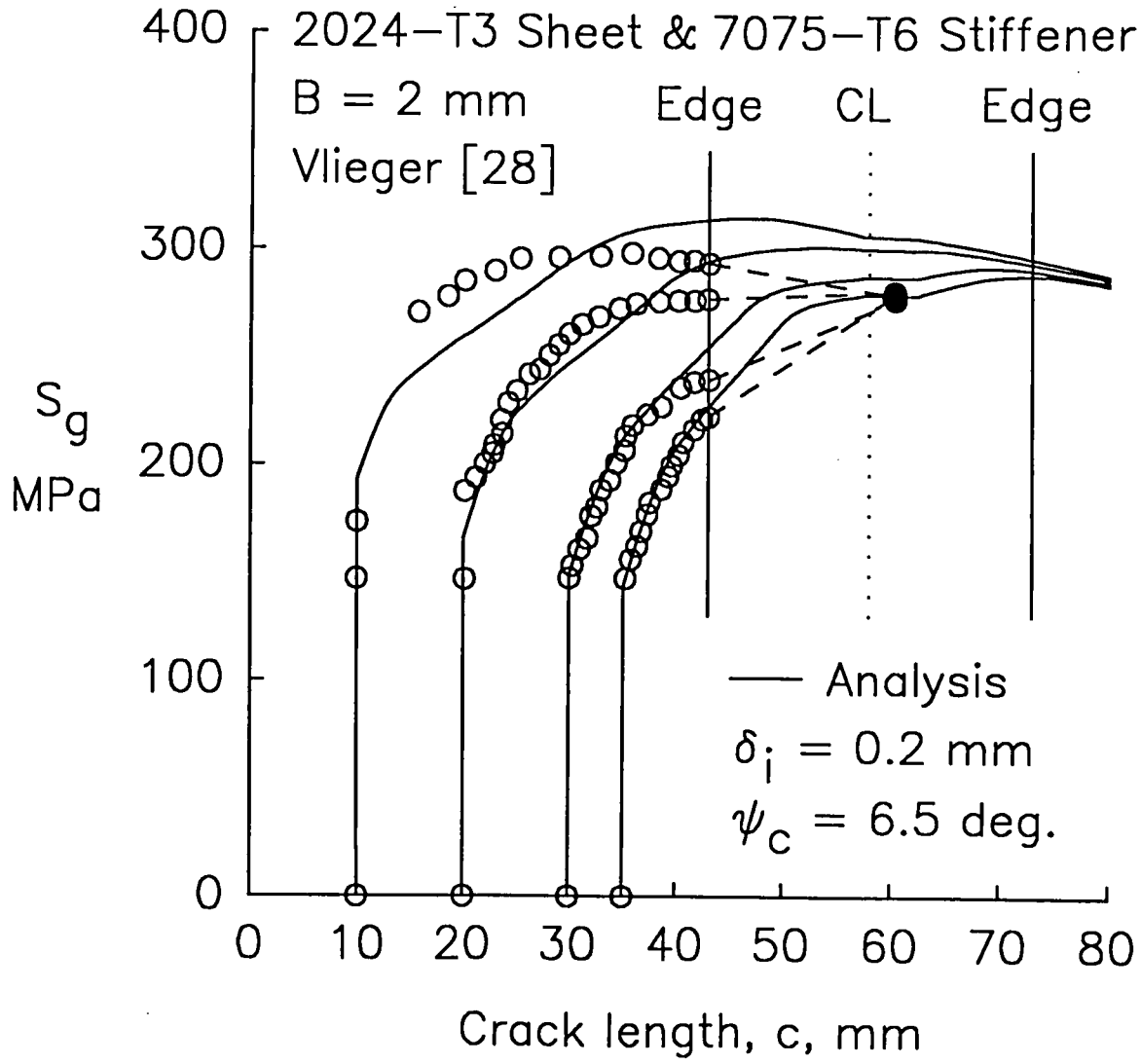

Figure 16 - Measured and predicted stable tearing in multiple stiffened sheets with a broken central stiffener.

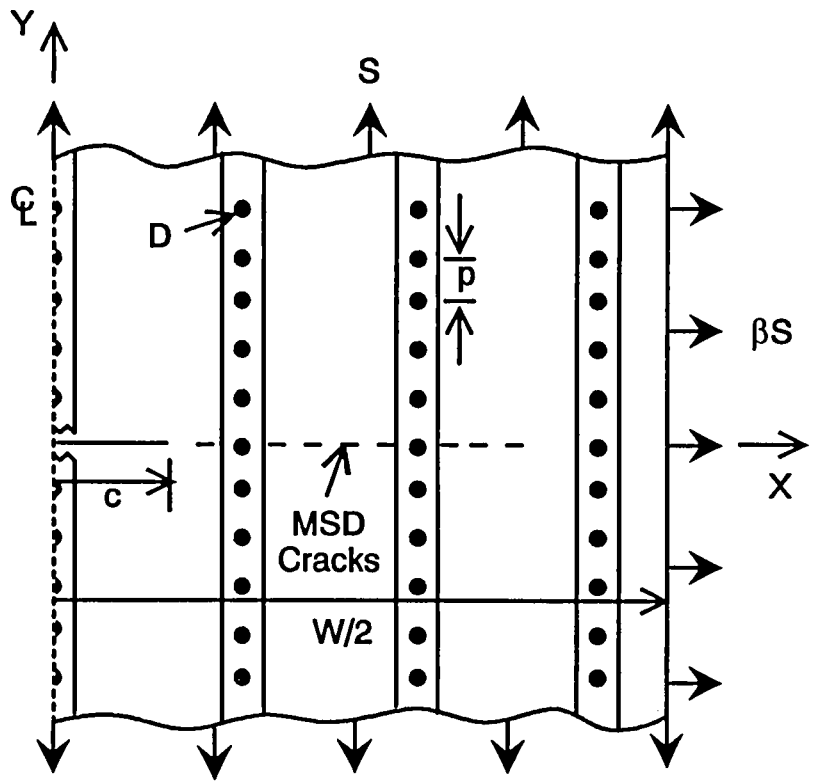

Figure 17 - Biaxially-loaded cracked stiffened panel with MSD.

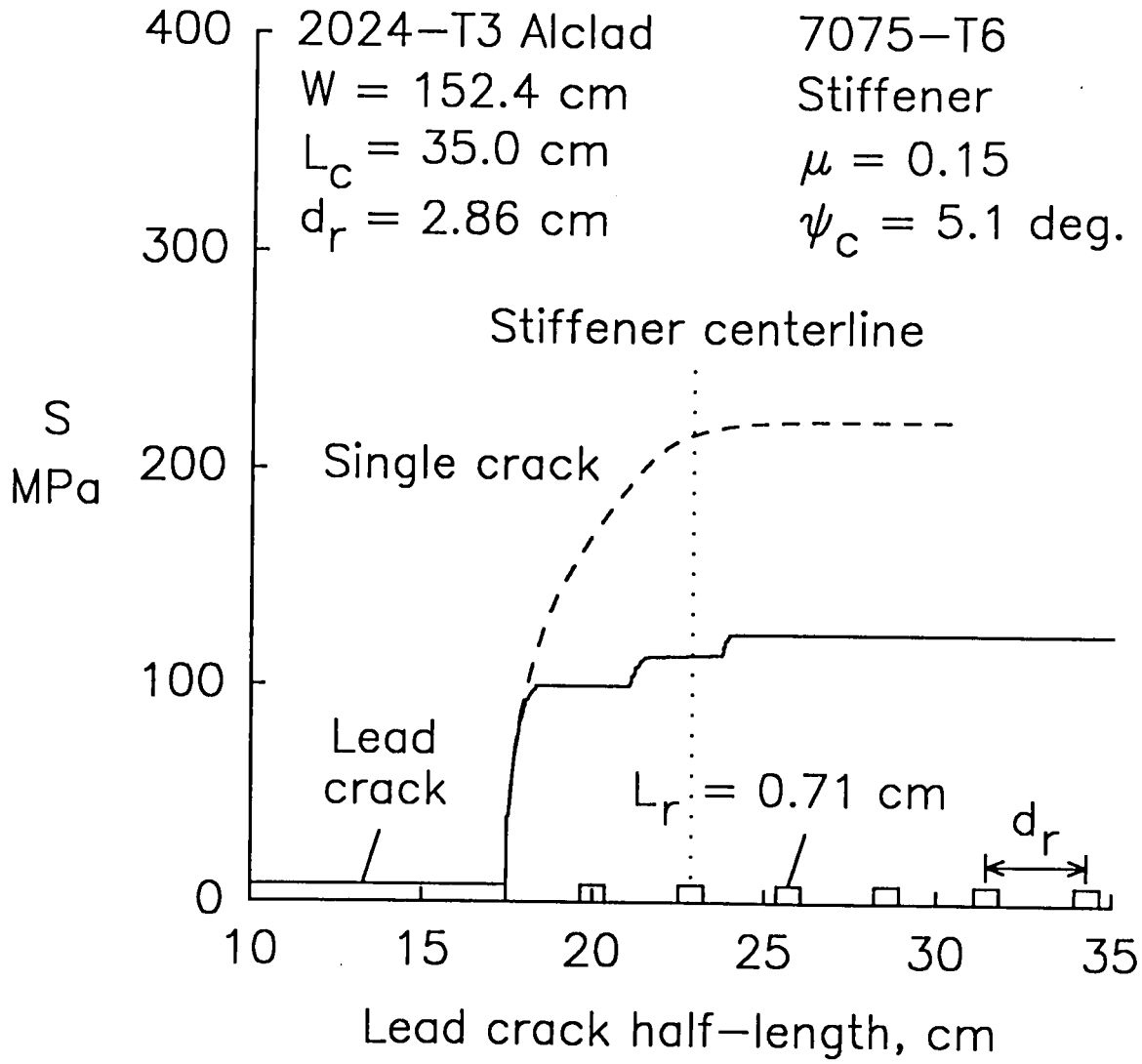

Figure 18 - Influence of stiffener on lead crack behavior for single and MSD cracking.

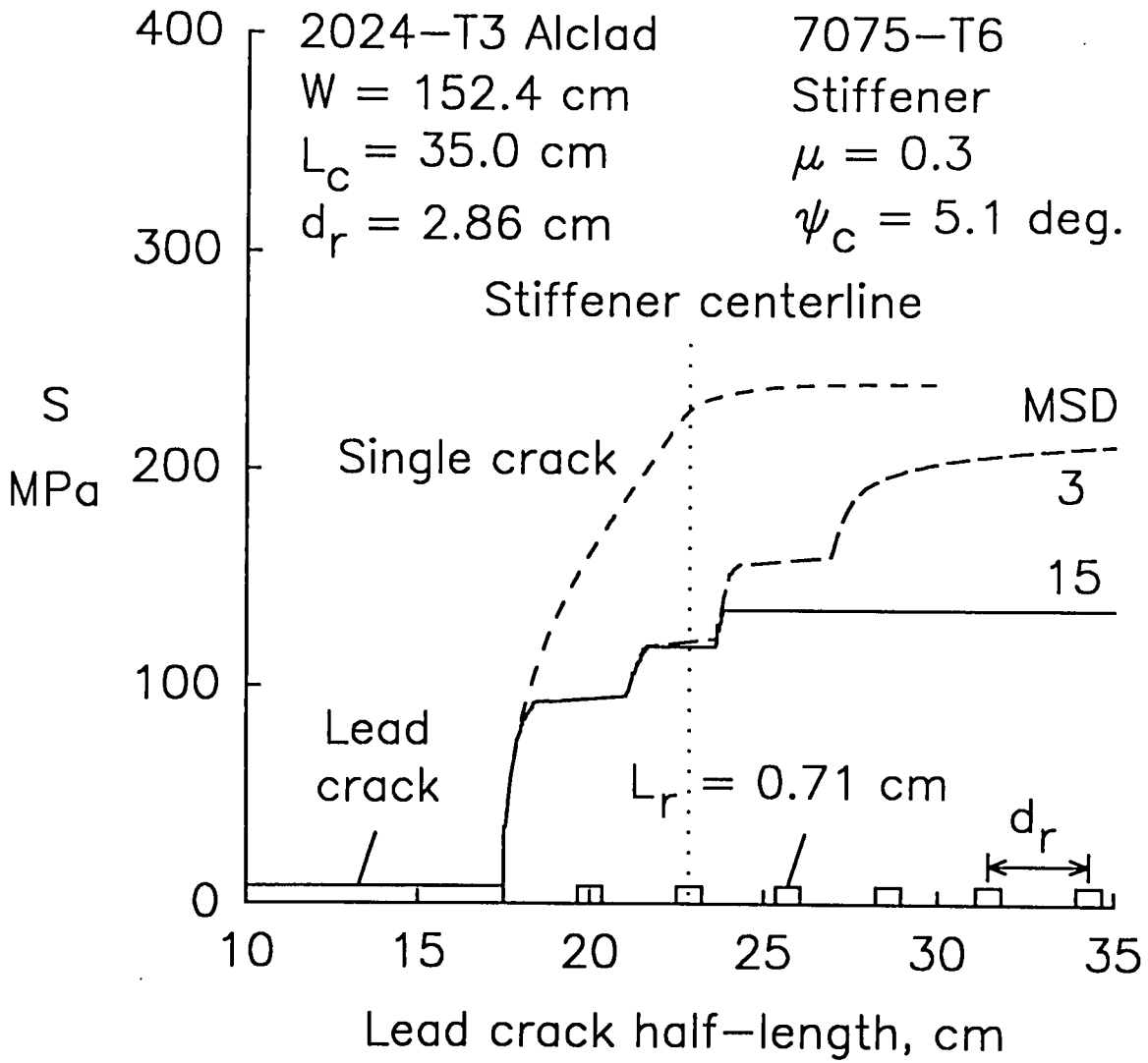

Figure 19 - Influence of stiffener on lead crack behavior for various number of MSD cracks.

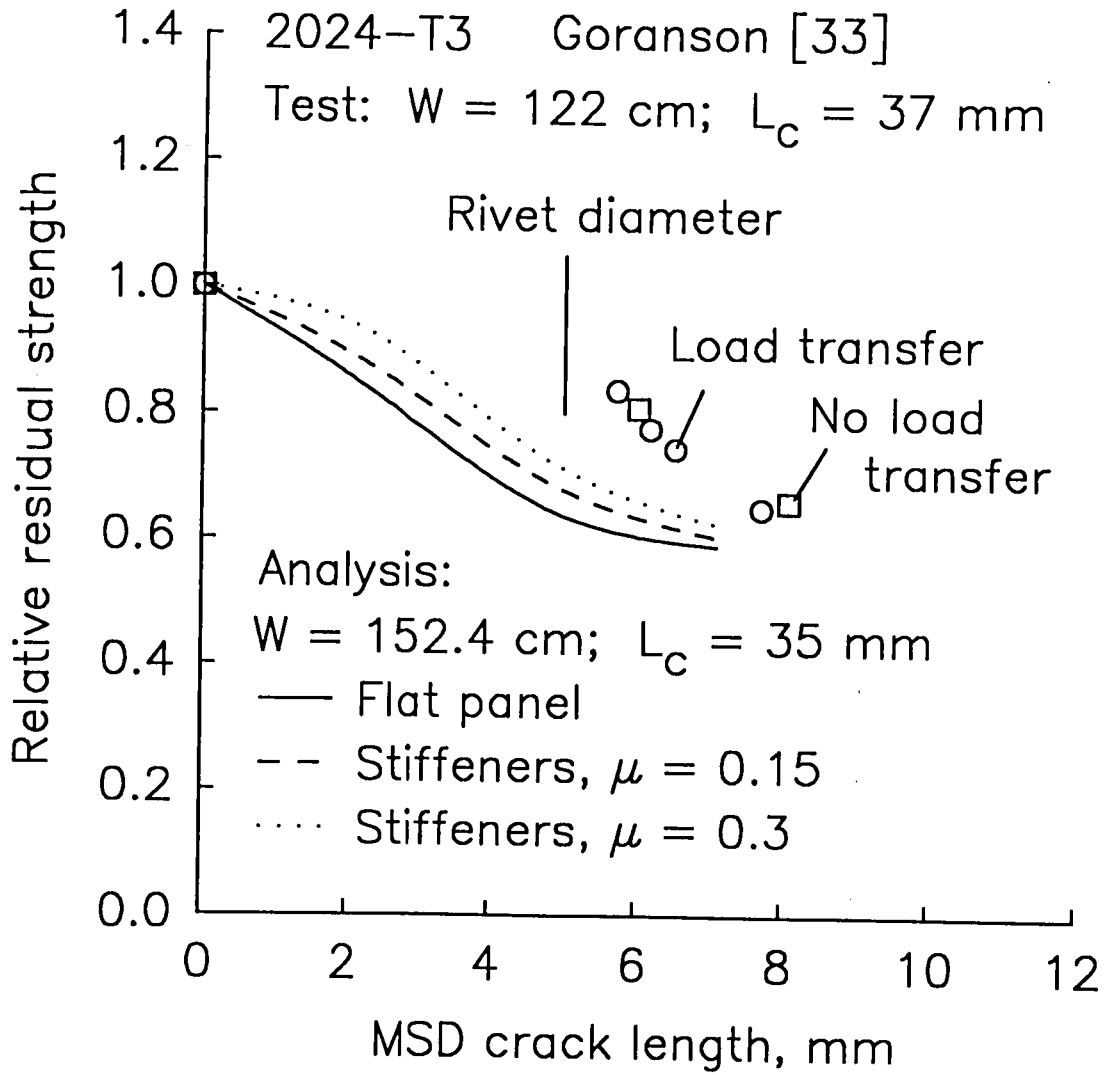

Figure 20 - Influence of stiffeners and MSD crack size on relative residual strengths.

REPORT DOCUMENTATION PAGE

Form Approved
OMB No. 0704-0188

1. AGENCY USE ONLY (*Leave blank*)	2. REPORT DATE	3. REPORT TYPE AND DATES COVERED
	October 1995	Technical Memorandum

4. TITLE AND SUBTITLE
Fracture Analysis of Stiffened Panels Under Biaxial Loading with Widespread Cracking

5. FUNDING NUMBERS
WU 538-02-10-01

6. AUTHOR(S)
J. C. Newman, Jr.

7. PERFORMING ORGANIZATION NAME(S) AND ADDRESS(ES)
NASA Langley Research Center
Hampton, VA 23681-0001

8. PERFORMING ORGANIZATION REPORT NUMBER

9. SPONSORING / MONITORING AGENCY NAME(S) AND ADDRESS(ES)
National Aeronautics and Administration
Washington, DC 20546-0001

10. SPONSORING / MONITORING AGENCY REPORT NUMBER
NASA TM-110197

11. SUPPLEMENTARY NOTES
Newman: Langley Research Center, Hampton, VA.

12a. DISTRIBUTION / AVAILABILITY STATEMENT
Unclassified - Unlimited

Subject Category 24

12b. DISTRIBUTION CODE

13. ABSTRACT (*Maximum 200 words*)

An elastic-plastic finite-element analysis with a critical crack-tip opening angle (CTOA) fracture criterion was used to model stable crack growth and fracture of 2024-T3 aluminum alloy (bare and clad) panels for several thicknesses. The panels had either single or multiple-site damage (MSD) cracks subjected to uniaxial or biaxial loading. Analyses were also conducted on cracked stiffened panels with single or MSD cracks. The critical CTOA value for each thickness was determined by matching the failure load on a middle-crack tension specimen. Comparisons were made between the critical angles determined from the finite-element analyses and those measured with photographic methods. Predicted load-against-crack extension and failure loads for panels under biaxial loading, panels with MSD cracks, and panels with various number of stiffeners were compared with test data, whenever possible. The predicted results agreed well with the test data even for large-scale plastic deformations. The analyses were also able to predict stable tearing behavior of a large lead crack in the presence of MSD cracks. The analyses were then used to study the influence of stiffeners on residual strength in the presence of widespread fatigue cracking. Small MSD cracks were found to greatly reduce the residual strength for large lead cracks even for stiffened panels.

14. SUBJECT TERMS
Cracks; Finite-element method; Stiffened panels; Plasticity; Fracture; Biaxial loading

15. NUMBER OF PAGES
37

16. PRICE CODE
A03

17. SECURITY CLASSIFICATION OF REPORT	18. SECURITY CLASSIFICATION OF THIS PAGE	19. SECURITY CLASSIFICATION OF ABSTRACT	20. LIMITATION OF ABSTRACT
Unclassified	Unclassified		